Title: CFD modeling of catalytic reactions in open-cell foam substrates

Author: A. Della Torre F. Lucci G. Montenegro A. Onorati P. Dimopoulos Eggenschwiler E. Tronconi G. Groppi

PII: S0098-1354(16)30127-2
DOI: http://dx.doi.org/doi:10.1016/j.compchemeng.2016.04.031
Reference: CACE 5450

To appear in: *Computers and Chemical Engineering*

Received date: 5-11-2015
Revised date: 4-4-2016
Accepted date: 19-4-2016

Please cite this article as: A. Della Torre, F. Lucci, G. Montenegro, A. Onorati, P. Dimopoulos Eggenschwiler, E. Tronconi, G. Groppi, CFD modeling of catalytic reactions in open-cell foam substrates, *<![CDATA[Computers and Chemical Engineering]]>* (2016), http://dx.doi.org/10.1016/j.compchemeng.2016.04.031

Highlights:

- We describe the implementation of a CFD model for the simulation of reacting flows through catalyzed porous substrates.
- We validate the model on the basis of previous experimental works available in the literature.
- The numerical model has been applied to investigate the physical phenomena occurring at the micro-scale of open-cell foams.
- Light-off curve for CO combustion was computed in case of foam-type reactor under different operating conditions.

CFD modeling of catalytic reactions in open-cell foam substrates

A. Della Torre[a,1,*], F. Lucci[b], G. Montenegro[a], A. Onorati[a], P. Dimopoulos Eggenschwiler[b], E. Tronconi[a], G. Groppi[a]

[a] *Politecnico di Milano, Department of Energy, via Lambruschini 4, 20156, Milano, Italy*
[b] *Laboratory for I.C. Engines, EMPA, Swiss Federal Laboratories for Materials Testing and Research, Dübendorf, Switzerland*

Abstract

Open cell foams are regarded with interest for applications as catalytic substrates for combustion, reformers and after-treatment converters for the pollutant emissions control. In this context, CFD represents a reliable and convenient tool for investigating and understanding the physical phenomena occurring at the micro-scale, in order to design and optimize these substrates. A CFD model for the simulation of the catalytic reactions occurring over the surface of open-cell foams is implemented and validated. The approach is based on a coupled finite-volume / finite-area strategy capable to describe the fluid-dynamic and the chemical phenomena occurring in both the fluid phase and solid phases. The adsorption/desorption of the reactants on the active sites and the surface reaction is modeled on the basis of a Langmuir-Hinshelwood mechanism. The model is able to describe the reactants conversion under both kinetics and diffusion control, allowing to predict the light-off curve characterizing the catalyst-coated foam substrate.

Keywords: open-cell foams, CFD, mass-transfer, surface reactions, Kelvin-cell

1. Introduction

Open-cell foams are cellular materials consisting of interconnected solid struts which form multiple pseudo-spherical void spaces. These spaces, named cells, *represent pores and are connected with each other by means of windows*, which allow the passage of the fluid through the structure. Foams can be made of different materials, metallic or ceramic, and are characterized by light-weight, high specific surfaces and high permeability to the fluid flow. These properties make foams suitable for a wide range of engineering applications, including: structural applications, mechanical energy absorbers, filtering devices and pneumatic silencers. With specific regard to the energy field, open-cell foams have attracted interest for heat transfer applications, e.g for the design of compact heat exchangers [1], or as catalytic substrates for combustion devices [2], fuel reforming systems and after-treatment converters for the pollutant emissions control [3, 4]. For these applications, the adoption of open-cell foams seems to be particularly convenient, since the tortuous flow path induced by their micro-structural geometry results in high activity per unit volume. Some previous works [5, 6, 7] compared the performances of open-cell foams and standard honeycombs substrates for automotive applications, pointing out that foams have promising strength points. These are basically related to the enhancement of the flow mixing and, therefore, of the mass-transfer properties, which allows to reach the same reactants conversion with only a fraction of the catalytic surface if compared to honeycombs. This primarily means an advantage in terms of a lower amount of noble metal to be loaded on the surface, which determines a reduction of the cost of the device. Furthermore, better performances are observed also in terms of a reduction of the ratio between pressure drop and reactant conversion.

From a literature survey, it results that the properties of foams have been experimentally investigated in several works and correlations for the pressure drop *[8, 38]* , heat-transfer [5, 9] and mass-transfer have been proposed [10, 11]. Along with experimental investigations, CFD approaches have been applied in order to enhance the understanding of the physical phenomena occurring at the micro-scale. In particular, DNS simulations have been adopted in order to characterize the flow regimes inside ideal foam structures, describing the transition from the laminar to the fully-turbulent regime [12]. Moreover, RANS simulations have been shown to be reliable tools for investigating the effects of geomet-

*Corresponding author
Email address: augusto.dellatorre@polimi.it (A. Della Torre)
[1]phone: +39 0223998631

rical parameters of the foam micro-structure (cell size, porosity) on its permeability *[12, 13]* , heat-transfer [14, 15, 16] , mass-transfer [17] and chemical conversion [18] properties. With regards to the CFD modeling of the reactions occurring over the catalytic surface of foam substrates, previous works focused on the characterization of species mass-transfer towards the active surface under the hypothesis of diffusion limited process. This assumption implies that the catalytic reactions are infinitely fast, so that the reactants are instantaneously converted into products as soon as they reach the surface. However, the chemical kinetics depend on the catalyst temperature according to an Arrhenius-like relation, therefore the assumption of infinitely fast reaction is realistic only when the temperature is sufficiently high. On the other hand, at low temperature, the conversion is limited by the chemical kinetics and suitable reaction models need to be introduced. In particular, this becomes mandatory when the light-off conversion properties of the substrate should be evaluated, as for the case of after-treatment systems developed for automotive applications, for which the pollutant abatement during the cold start phase is a crucial aspect. In this scenario, the micro-scale CFD simulation of the reactive flow inside of the substrate can provide a deeper understanding of the conversion mechanism, giving useful information for the optimization of the morphological and geometrical parameters of the coated substrate. Moreover, it can be regarded as a support tool for the development of macro-scale simplified numerical models, based on 0D or 1D approaches [19, 20], which can be employed for the simulation and the optimization of catalytic devices.

The modeling of the chemical reactions occurring on a generic catalytic surface can be addressed following different approaches, characterized by an increasing level of detail and computational effort. The most accurate approach is based on the adoption of detailed micro-microkinetic models for the description of the elementary reaction steps occurring on the catalyst surface [21, 22]. The coupling of the detailed heterogeneous micro-microkinetic model to the CFD is a particularly challenging task, due to the stiffness and the high non-linearities of the equations. Among all the methods which can be adopted for the coupling, the most attractive alternatives are the fully-coupled algorithms [23] and the segregated algorithms based on operator-splitting methods [24]. The latter approach is particularly efficient, since it reduces the size of the system of equations to be solved resulting in a lower computational effort compared to fully-coupled algorithm, as pointed out in [25]. The adoption of a detailed microkinetic model is mandatory when the purpose of the analysis is the evaluation of the influence of the catalyst composition on the surface reactivity. On the other hand, when the characterization of the surface reactivity is already available (e.g. by means of experimental measurements), simplified reaction models can be applied, with a significant reduction of the computational effort. These models (e.g. Languimir-Hinshelwood) describe the macroscopic functionality of the catalyst on the basis of the surface conditions in terms of temperature, pressure and composition, without the need of solving the detailed micro-kinetic equations governing the conversion mechanism. This approach is particularly convenient when the focus of the analysis is the study of the performances of a particular catalyzed substrate, in order to investigate the effects of different operating conditions and/or geometrical parameters. According to this purpose, the detailed insight into the chemical process provided by a micro-microkinetic model can be considered unnecessary, not justifying the related additional computational burden.

This second approach has been followed in this work to develop a CFD model for the study of the performances of open-cell foam substrates, taking into account the dependency of the surface reactivity on the temperature, in order to describe the substrate behavior during the light-off. The model has been proved to be able to describe the conversion under both kinetic-controlled and diffusion-controlled regimes. The parameters of the model were chosen on the basis of the values experimentally determined in the literature for similar catalyst. The validation of the implemented CFD framework was addressed by comparing the results of the simulations with experimental data. In particular, comparisons were made simulating at first a single channel of a plate-type reactor and then considering a more complex foam-type reactor for which the light-off curve was calculated under different operating conditions.

2. CFD model

The CFD model developed in this work is based on the open-source finite volume code OpenFOAM® [26, 27]. This was extended by means of the implementation of a specific library for the simulation of catalytic surface reactions. In particular, the structure of the model consists of two main cores: a) a finite volume (FV) solver, which describes the fluid-dynamic and the chemistry phenomena occurring in the fluid phase and b) a finite area (FA) solver which describes the phenom-

ena related to the catalytic species conversion occurring on the washcoat surface.

2.1. FV solver

The FV model is based on the solution of the conservation equations of mass, momentum, energy and species:

- mass:

$$\frac{\partial \rho}{\partial t} + \nabla \cdot (\rho \mathbf{U}) = 0 \tag{1}$$

- momentum:

$$\frac{\partial \rho \mathbf{U}}{\partial t} + \nabla \cdot (\rho \mathbf{U}\mathbf{U}) = \rho \mathbf{g} - \nabla \left(p + \frac{2}{3}\mu \nabla \cdot \mathbf{U} \right) + \nabla \cdot \left[\mu \left(\nabla \mathbf{U} + \nabla \mathbf{U}^T \right) \right] \tag{2}$$

- energy:

$$\frac{\partial \rho e}{\partial t} + \nabla \cdot (\rho e \mathbf{U}) = \rho \mathbf{g}\mathbf{U} - \nabla \cdot (p\mathbf{U}) - \nabla \cdot \left[\frac{2}{3}\mu (\nabla \cdot \mathbf{U}) \mathbf{U} \right] + \nabla \cdot \left[\mu \left(\nabla \mathbf{U} + \nabla \mathbf{U}^T \right) \mathbf{U} \right] + \nabla \cdot (\lambda \nabla T) + \rho Q + \mathfrak{Q}^{f \to w} \tag{3}$$

- species:

$$\frac{\partial \rho Y_i}{\partial t} + \nabla \cdot (\rho Y_i \mathbf{U}) = -\nabla \cdot (\rho \mathfrak{D}_i \nabla Y_i) + \rho R + \mathfrak{R}_i^{f \to w} \tag{4}$$

The set of equations is then closed by the perfect gas equation of state. The thermal properties of the multicomponent mixture are determined on the basis of the JANAF tables. A Sutherland model is applied for the calculation of the transport properties, in order to take into account the dependency of viscosity on the gas temperature. The mass diffusivity is modeled under the assumption of Schmidt number equal to 1 in order to reduce the computational burden. However, this assumption is removed for the calculation of the species diffusion coefficient in the near-wall region by means of the FA solver. With regard to the gas phase chemistry modeling, an Arrhenius-type expression is adopted to determine the reaction rates.

The FV solver is coupled to the FA solver by means of the source terms $\mathfrak{Q}^{f \to w}$ and $\mathfrak{R}_i^{f \to w}$, which take into account the energy and species transfer occurring between the boundary cells and the washcoat surface.

2.2. FA solver

The conversion of reactants into products involves their convective mass-transfer towards the catalytic surface of the washcoat, as well as adsorption of reactants and desorption of products at the active sites. Moreover, as a consequence of the reactions, heat is released and accumulated in the substrate and transferred to the fluid phase. In order to take into account these phenomena, the FA solver is based on three different submodels: a) diffusion model, b) reaction model and c) heat-transfer model.

The diffusion model describes the mass transfer between the fluid and the washcoat surface. For each species, the diffusive flux has been modeled on the basis of the Fick's law, leading to:

$$J_i = M_i \mathfrak{D}_i \frac{C_{f,i} - C_{w,i}}{\Delta L}, \tag{5}$$

where ΔL *is the mesh size and* $\mathfrak{D}_i$ *is the diffusion coefficient for one component in a mixture, given by:*

$$\mathfrak{D}_i = \frac{1 - C_i}{\sum_{j \neq i} \frac{C_i}{\mathfrak{D}_{i,j}}}. \tag{6}$$

The binary gas diffusion coefficient $\mathfrak{D}_{i,j}$ is calculated by means of the Chapman-Enskog equation:

$$\mathfrak{D}_{ij} = 1.85 \cdot 10^{-3} \frac{T^{1.5} \left(\frac{1}{M_i} + \frac{1}{M_j} \right)^{0.5}}{p \left(\frac{\sigma_i + \sigma_j}{2} \right)^2 \Omega_D}, \tag{7}$$

where Ω_D is the collision integral, evaluated on the basis of the Lennard-Jones potential (ϵ_0), and σ_i is the Lennard-Jones collision diameter *[29] . The washcoat model adopted in this work is based on a zero-dimensional approximation, assuming the reacting layer thickness as infinitely small and neglecting the variation of the species mass fractions along the direction normal to the fluid-solid interface. However, in order to describe the effects of the species diffusion into the washcoat, this computational framework can be extended by means of the implementation of additional models, based on both zero- or one-dimensional assumption, which can be found in the literature [30, 31].*

The reaction submodel describes the species conversion occurring on the catalytic surface. In order to account for the competition of the chemical species on the active sites, the Langmuir-Hinshelwood theory has been adopted. For a generic reaction:

$$\alpha A + \beta B \rightarrow \gamma C + \delta D, \tag{8}$$

the reaction rate can be expressed as follows:

$$r_i = k_{r,i} \frac{C_{s,A} C_{s,B}}{G_i} \left(1 - \frac{C_{s,C}^{\gamma} C_{s,D}^{\delta}}{C_A^{\alpha} C_B^{\beta} K_p(T)} \right). \tag{9}$$

The term G_i is the inhibition factor, which takes into account the impact on the overall kinetics of the adsorption and desorption of reactants and products on the ac-

tive sites. This term is directly proportional to the concentration of the reactants involved in the reactions:

$$G_i = (1 + k_{a,1}C_{s,A} + k_{a,2}C_{s,B})^2 \tag{10}$$

The terms $k_{r,i}$ and $k_{a,i}$ are Arrhenius type kinetic constants which regulate the reaction and the adsorption mechanisms:

$$k_{r,i} = A_{r,i}\, exp\left(-\frac{E_{r,i}}{RT_w}\right), \tag{11}$$

$$k_{a,i} = A_{a,i}\, exp\left(-\frac{E_{a,i}}{RT_w}\right). \tag{12}$$

The heat-transfer submodel calculates the heat exchanged between the washcoat surface and the fluid. The heat flux is determined as:

$$Q^{f\to w} = h\frac{A}{V}\left(T_f - T_w\right), \tag{13}$$

where the convective coefficient h is equal to $k_f/\Delta L$ in the laminar case or it is calculated from the turbulent Prandtl as $(c_p\mu_t)/(\Delta L Pr_t)$ in case of turbulent boundary layers.

On the basis of these submodels, a possible approach for the simulation of the phenomena occurring on the washcoat is to solve the balance equations for both the species mass and the energy, taking into account their eventual accumulation:

$$\frac{\partial m_{w,i}}{\partial t} = J_i - r_i, \tag{14}$$

$$\frac{\partial \rho_w c_w T_w}{\partial t} = Q^{f\to w} + H_r. \tag{15}$$

These are two ordinary differential equations which can be solved by means of suitable algorithms (e.g. Runge-Kutta) in order to get, at each fluid-dynamic time-step, the values of the source terms $\mathfrak{R}_i^{f\to w}$ and $\mathfrak{Q}^{f\to w}$ included in the equations 3 and 4 solved by the FV solver. However, this solution approach has some limitations when the purpose of the simulation is to investigate steady-state regime condition. As a matter of fact, since it requires a time discretization in order to evolve the solution, it cannot be coupled to the standard pressure-based FV solvers based on the SIMPLE algorithm [28]. In this case, Eqns. 14 and 15 should be solved implicitly with an iterative procedure. However, in order to keep the computational effort low, an alternative simplified procedure has been implemented on the basis of the Baruah's theory [32]. The main assumption is that when the global kinetics becomes controlled by the mass transfer process, all the reactants diffusing into the washcoat are supposed to react on the active sites and consequently their concentration in the solid phase can be considered small. This means that the concentration gradient between the gas phase and the solid phase of the reactants can be approximated by the gas phase concentration itself. Therefore, the species conversion source term $\mathfrak{R}_i^{f\to w}$ in Eq. 4 is evaluated by limiting the reaction rate expressed by the Langmuir-Hinshelwood expression (Eq. 9) on the basis of the reactants diffusion flux (Eq. 5):

$$\mathfrak{R}_i^{f\to w} = \frac{A}{V}\begin{cases}\sum_j \alpha_{i,j} r_j, & \text{if } J_i > \sum_j \alpha_{i,j} r_j \\ J_i & \text{if } J_i < \sum_j \alpha_{i,j} r_j\end{cases} \tag{16}$$

In this way, at low temperature, when the washcoat temperature T_w is lower than the ligh-off temperature, the species conversion is limited by the reaction kinetics; conversely, at high temperature, the diffusion of the reactants represents the limiting factor.

In order to guarantee the stability of the solution procedure, a specific numerical treatment has been adopted for the coupling of the FV and FA solver. In particular, the source terms of energy $\mathfrak{Q}^{f\to w}$ and species $\mathfrak{R}_i^{f\to w}$ are included in Eqns. 3 - 4 by means of a semi-implicit approach. Considering the generic system describing a transport equation:

$$\mathbf{A}\,\mathbf{x} = \mathbf{b}\,, \tag{17}$$

the generic source term $\mathbf{S}$ is split into two contributions, expliciting the linear dependency with respect to $\mathbf{x}$:

$$\mathbf{S} = \mathbf{S_A}\mathbf{x} + \mathbf{S_b}\,, \tag{18}$$

where $\mathbf{S_A}$ is a diagonal matrix. Therefore, the source term can be included in the original system as:

$$(\mathbf{A} - \mathbf{S_A})\,\mathbf{x} = \mathbf{b} + \mathbf{S_b}\,. \tag{19}$$

Since a part of the source term is included in the diagonal of the coefficient matrix, and therefore is treated implicitly, the stability of the solution algorithm is increased, allowing to perform the CFD simulation in presence of chemical reactions with both transient and steady-state approaches.

3. Numerical simulations

The CFD model has been validated resorting to two different experimental configurations. The first (Figure 1) is a metallic plate-type reactor [33], consisting of four slabs assembled with spacers in order to form three parallel rectangular channels (width = 46 mm, length = 200 mm). In order to reduce the computational cost of the CFD simulation, some reasonable assumptions were introduced. In particular, a single channel was considered and a 2D approximation was adopted. The computational mesh was refined near the walls (Figure 2), in order to accurately resolve the velocity profile and the mass transfer occurring at the boundary layer region.

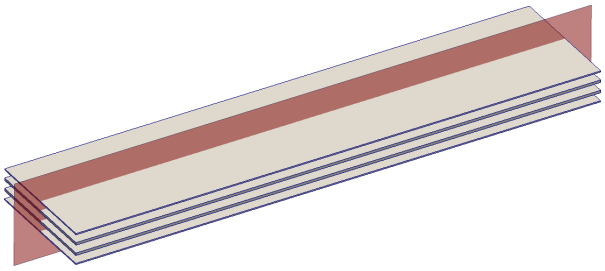

Figure 1: Schematic of the plate-type reactor configuration: four slabs are assembled to form three parallel rectangular channels. A single 2D channel, located on the middle plane (highlighted in red), was considered in the simulations.

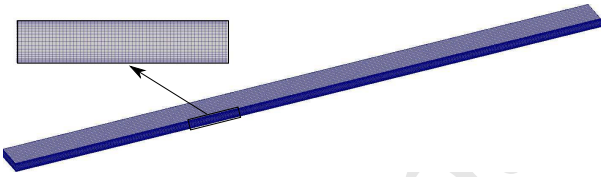

Figure 2: 2D mesh of a single channel of the plate-type reactor. The zoom shows the details of the mesh in the boundary layer region.

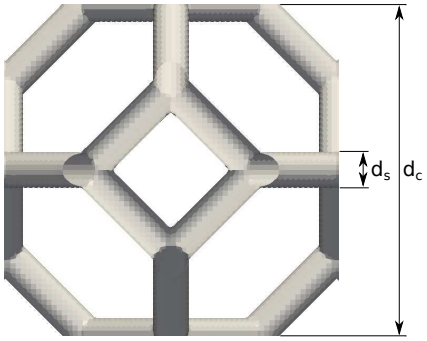

Figure 3: Schematic of a single Kelvin-cell, highlighting the main characteristic dimension of the structure.

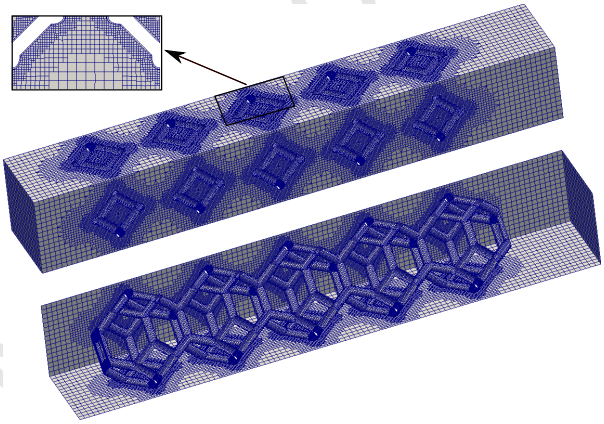

Figure 4: Computational mesh for the foam-type reactor configuration. The zoom shows the details of the mesh in the boundary layer region.

The second validation case consists of a set of open-cell foam samples having different properties in terms of pore density and porosity. The properties of these foams [10] are listed in Table 1. The foam micro-structural geometry is approximated as a Kelvin-cell structure, as shown in Figure 3. The main geometrical parameters of the Kelvin-cell structure have been chosen in such a way to match the porosity and the specific surface of the samples. Five Kelvin-cells were grouped together along the axial direction in order to reconstruct a foam sample having a length of 6 *mm*.

The computational mesh has been generated with the `snappyHexMesh` utility included in OpenFOAM. This is a fully-automatic cartesian mesh generator based on the octree concept and it creates a high quality mesh which is predominantely hexaedral, with a small percentage of tetrahedral/polyhedral cells concentrated in the near-wall region. As shown in Figure 4, boundary layer has been added near the walls, in order to allow a better discretization of the species concentration and temperature gradients close to the washcoat surface.

Steady-state simulations were run for both the two configurations adopting the SIMPLE (Semi-Implicit Method for Pressure Linked Equations) algorithm [28]. At the outlet section a Dirichlet boundary condition has been assigned to the pressure field, whereas Neumann-type boundary condition has been used for the velocity, temperature and species mass-fraction fields. At the inlet Neumann condition has been imposed for the pressure field, while mass flow, temperature and species mass-fraction were uniformly assigned with a specific value. Symmetry boundary conditions were applied on the lateral faces of the Kelvin-cell structure domain. The temperature distribution inside the catalyst substrate (plates or foam) was assumed to be isothermal (i.e. the thermal conductivity of the substrate is sufficiently high to guarantee an efficient heat removal from the reacting zones), therefore a fixed temperature has been imposed on the catalytic surface.

Table 1: Properties of the foams with different pore density and porosity.

Sample	Foam Porosity [-]	Cell density [ppi]	$S_V[m^2/m^3]$	Kelvin cell model $d_c[m]$	$d_s[m]$
A	0.945	5.9	665.3	$3.16 \cdot 10^{-3}$	$3.04 \cdot 10^{-4}$
B	0.927	5.4	703.6	$3.36 \cdot 10^{-3}$	$3.77 \cdot 10^{-4}$
C	0.938	11.5	1445.1	$1.53 \cdot 10^{-3}$	$1.57 \cdot 10^{-4}$
D	0.937	12.8	1543.3	$1.44 \cdot 10^{-3}$	$1.49 \cdot 10^{-4}$
E	0.932	15.0	1827.4	$1.26 \cdot 10^{-3}$	$1.36 \cdot 10^{-4}$

4. Kinetic parameters

In this study the catalytic combustion of CO was considered:

$$2CO + O_2 \rightarrow 2CO_2. \tag{20}$$

For both the plate-type and the foam reactors, the catalytic washcoat consists of palladium oxide supported on γ-alumina. In case of plate-type reactor, the specific loading of $\gamma - Al_2O_3$ was $6.9\,mg/cm^3$, resulting in an average washcoat thickness of $60\,\mu m$. On the other hand, in case of foams, the loading was around $2-3\,mg/cm^3$ determining an average coating thickness of $21\,\mu m$. In both cases, the percentage of catalyst was estimated as 3% (w/w) palladium over γ-alumina. Further details about the properties of the catalytic layer and the procedure adopted for its deposition can be found in [34, 35]. The performance of the catalytic washcoat in terms of molar rate of species conversion with respect to the catalytic surface was experimentally investigated in [34], proposing the following rate equation in case of CO oxidation:

$$r = k_r \frac{p_{CO} p_{O_2}^{1/2}}{(1 + k_a p_{CO})^2} \left[\frac{mol}{m^2 s}\right]. \tag{21}$$

In this expression the Arrenius-type temperature dependency of the kinetic coefficients is parametrised on the basis of four constant estimates, determined by means of non-linear regression on measured data:

$$k_r = \exp\left[0.65 - 4.13\left(\frac{1000}{T_w} - \frac{1000}{473}\right)\right], \tag{22}$$

$$k_a = \exp\left[4.44 + 4.79\left(\frac{1000}{T_w} - \frac{1000}{473}\right)\right]. \tag{23}$$

The kinetic parameters adopted in the CFD simulation were determined on the basis of this equation, in order to fit the Langmuir-Hinshelwood model (Eq. 9) to the experimental rate expression over the temperature range of interest. In particular, the following values for the constants included in Eqns. 11 and 12 were adopted: $A_r = 5.0 \cdot 10^9$, $E_r/R = 11700$, $A_a = 65$, $E_a/R = 961$.

5. Results and discussion

The validation of the implemented CFD models was performed in three steps, comparing the simulation results with the available experimental data. At first, the plate-type reactor was simulated, in order to predict the CO conversion in a condition in which the chemical reaction represents the bottleneck of the process. Once the reaction submodel was validated on this simple test case, different foam reactors were considered and simulations were performed at higher temperature levels, where the conversion process is limited by the diffusion of the reactants from the gas phase to the washcoat. Finally, the calculation of the entire light-off curve was addressed, in order to verify the capability of the model to predict both the conversion limitation given by the chemical kinetics at low temperature and by the mass-diffusion at high temperature.

For the case of the plate-type reactor, simulations were run considering two CO feed concentrations ($Y_{CO} = 3.5\%$ and $Y_{CO} = 8.7\%$) and two feed flow rates ($Q = 500\,Ncc/min$ and $Q = 1000\,Ncc/min$). Under these conditions, as verified in a previous experimental study [33], the conversion of reactants into products is completely governed by the chemical kinetics, without any limitation related to the diffusion of species to the catalytic surface. Moreover, since the plate-type reactor has been proved to guarantee a good heat removal, in the simulations an isothermal condition has been adopted for the catalyst surface.

In Figure 5 the light-off curve for the case at lower flow rate is reported, showing a good agreement with the experimental data. The model is able to correctly describe the translation of the curve towards higher temperature levels when the CO feed concentration increases, as a consequence of the higher importance of the inhibition term in Eqn. 10, which determines a reduction of the reaction rate. In a similar way, Figure 6 shows an increase of the light-off temperature with the flow rate: this is related to the fact that, increasing the reactants flow rate, a higher reaction rate is needed to obtain the same conversion. Moreover, in this condi-

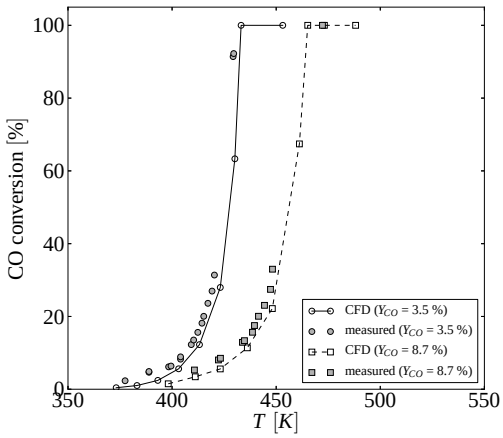

Figure 5: Plate-type reactor: CO conversion for a inlet feed flow rate $Q = 500\,Ncc/min$.

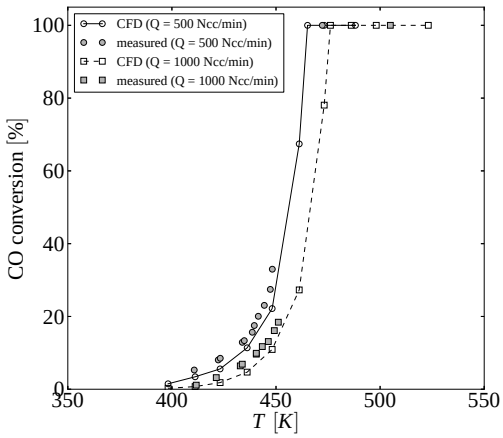

Figure 6: Plate-type reactor: CO conversion for a inlet CO mass fraction $Y_{CO} = 8.7\%$.

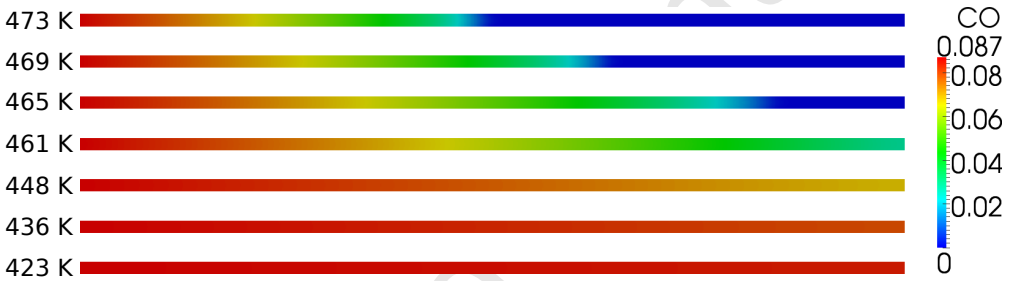

Figure 7: Plate-type reactor: CO field inside the channel for a inlet CO mass fraction $Y_{CO} = 8.7\%$ and a feed flow rate $Q = 500\,Ncc/min$.

tion, also the CO concentration on the catalytic surface becomes higher, increasing the value of the inhibition factor G_i and determining a further reduction of the catalytic activity. For temperatures higher than the light-off one, a full CO conversion is observed for all the operating conditions considered, due to the low velocity of the stream flowing in the reactor ($U = 0.05 \sim 0.1\,m/s$). In Figure 7 the CO mass fraction field in the channel for the case of $Q = 500\,Ncc/min$ and $Y = 8.7\%$ is reported for different temperatures. It can be seen that at the lowest temperature, which is below the light-off one, the conversion is negligible; increasing the temperature the conversion becomes significant and full conversion is achieved around 463K. Then, at higher temperatures, since the reaction is very fast and no diffusion limitation occurs, the CO conversion is completed after a certain distance from the inlet: in this condition just a portion of the channel participates to the catalytic reaction. *Moreover, it can be noticed that, as a consequence of the very low Reynolds number ($Re < 8$), the diffusive transport in the radial direction is so dominant that the radial variation of the species composition becomes negligible [39].*

As a further step of the validation, a set of foam-type reactors was considered [10]. In order to check if the Kelvin cell model adopted for the reconstruction of the micro-structure was appropriate to describe the fluid-dynamics inside the foams, pressure drop was calculated in case of a cold non-reacting flow. The comparison with the experimental measurements is reported in Figure 8 and shows a satisfactory agreement for low flow velocities (up to $5\,m/s$), whereas it can be noticed a slight underestimation of the pressure drop at the higher flow velocities. However, since the reactive tests were run with a maximum flow velocity lower than $5\,m/s$, the Kelvin cell approximation was considered acceptable according to the scope of this analysis. On the other hand, the underestimation at high velocity is related to a lower inertial contribution to the pressure drop (Forchheimer term), which can be explained with the different morphology of the Kelvin cell with respect to the actual foam micro-structure. In particular, this can be related

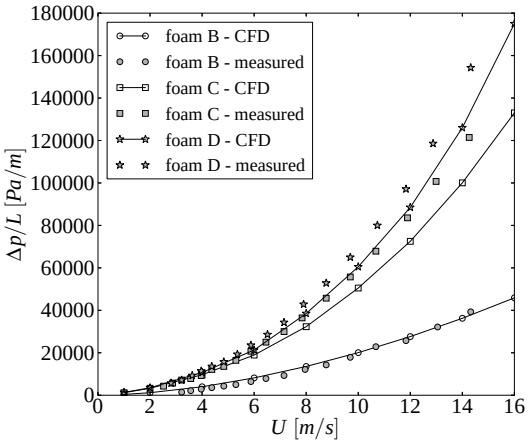

Figure 8: Foam-type reactor: pressure drop for different foam samples.

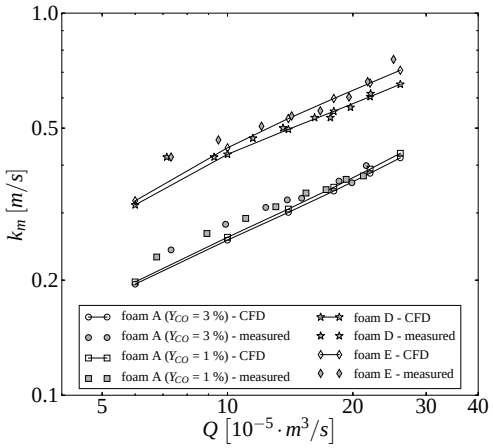

Figure 9: Foam-type reactor: mass-transfer coefficients for different foam samples.

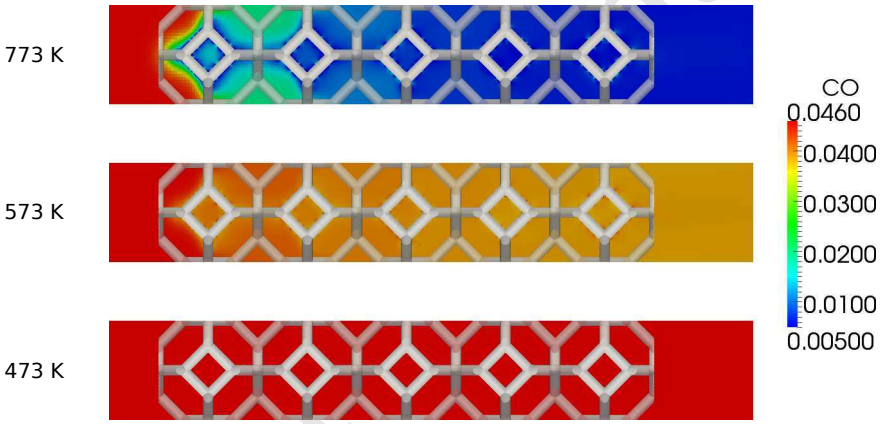

Figure 10: Foam-type reactor, sample E: CO field for an inlet CO mass fraction Y_{CO} = 4.6% and a feed flow rate $Q = 3000\,Ncc/min$. Field is shown on a plane located at the boundary of the domain (offset of $d_c/2$ with respect to the center of the Kelvin cell).

to a slight anisotropy of the considered foams and to the higher tortuosity of the real micro-structures [36, 37], which cannot be described by the standard Kelvin cell approximation adopted in this study. *A further reason for the underestimation of the pressure drop can be identified in the variability of the pore size of the real foam, as described in [38]: this means that, for a certain porosity and specific surface, a higher pore size variation determines a reduction of the permeability.*

Once the validity of the geometric reconstruction was proved, reactive simulations were run considering diffusion-controlled conditions. Mass-transfer coefficients k_m were estimated from the CO conversion η as:

$$k_m = -\frac{ln\,(1-\eta)}{S_V V/Q} \tag{24}$$

In Figure 9 the mass-transfer coefficients k_m are plotted versus the feed flow rate for different foam samples. The agreement with the experimental data can be regarded as good. The CFD simulations capture the increase of the mass-transfer coefficient when foams having small pore size are considered and correctly predict the dependency of k_m on the mass flow rate.

The light-off curve was calculated for the sample E, considering different flow rates ($Q = 3000\,Ncc/min$ and $Q = 6000\,Ncc/min$) and CO concentrations (Y_{CO} = 3% and Y_{CO} = 5%). Figure 10 shows the CO mass fraction field inside the foam for $Q = 6000\,Ncc/min$ and Y_{CO} = 5% considering three different temperatures. At the lowest one (473 K) the conversion is negligible, since the light-off of the mixture is not yet occurred. Then, for a certain range of temperature higher than the light-off one, the CO conversion increases proportion-

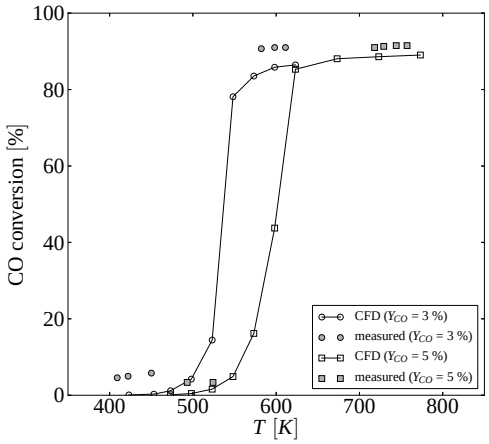

Figure 11: Foam-type reactor, sample E: CO conversion for an inlet feed flow rate $Q = 3000\,Ncc/min$.

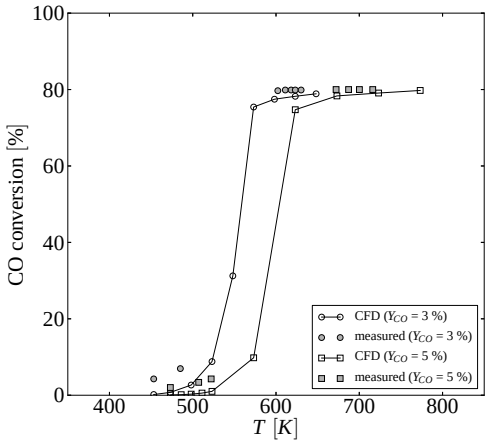

Figure 12: Foam-type reactor, sample E: CO conversion for an inlet feed flow rate $Q = 6000\,Ncc/min$.

ally to the reaction rate: an example of CO field in this condition is reported for T=573K. Finally, the limitation represented by the species diffusion becomes the bottleneck of the conversion process when the reaction rate becomes very high: as shown for T=773 K, under this condition the CO field exhibits significant gradients in the direction of the foam surface, which are responsible for its mass transfer towards the reaction region. It can be seen in Figures 11 and 12 that CFD simulations give a reasonable prediction of the light-off curve, describing the transition from a kinetic-controlled to a diffusion-controlled process.

The CO conversion at high temperature is correctly predicted, while an overestimation of the light-off temperature with respect to the measurements can be observed, in particular for the lower CO concentration. This can be explained considering the assumption, made in the simulations, of uniform temperature distribution on the foam catalyst surface. Actually, this assumption does not describe accurately the experimental condition under which measurements were performed. As a matter of fact, on the contrary of the plate-type reactor configuration, the foam-type one does not allow an efficient removal of the heat from the catalytic surface. Therefore, the temperature of the catalyst is expected to be higher than the temperature measured in the front of the foam, where the thermocouple is located. For this reason, the computed light-off curve is shifted towards higher temperatures, if compared to the measured one. In order to provide a better prediction of the light-off temperature, the thermal balance for the entire catalyst substrate should be considered, in such a way to determine the actual temperature distribution of the surface. In this case the substrate solid matrix, along with the enclosing duct, should be modeled and a more sophisticated conjugate heat-transfer approach should be employed.

It can be observed that the light-off temperature in case of the foam substrate is higher than the one in the case of plate-type reactor. This behavior can be explained considering that the velocity of the flow in the first case ($U = 1 \sim 5\,m/s$) is one order of magnitude higher than the second one ($U = 0.01 \sim 0.1\,m/s$) and therefore, a higher temperature is needed to establish a reaction rate sufficient to give an appreciable CO conversion. Additionally, as a result of the lower conversion, also the CO concentration on the catalytic surface increases, resulting in a higher value of the inhibition factor G_i, which further reduces the reaction rate.

Moreover, it can be seen that, at the light-off temperature, when the conversion is reaching its maximum value, the curve exhibits a smooth transition from kinetic- to diffusion-controlled CO conversion. As a matter of fact, the present model does not include a pore-diffusion sub-model, therefore a sharp transition should be expected in this region. However, in this case the explanation for the smoothness of the curve can be related to the entrance effects which occur at the foam front. As shown in Figure 13, the CO gradient in the first cell is more significant than in the downstream ones: this is due to the different morphology of the foam front and to the fact that no recirculation/stagnation zone are present. This means that also the specific CO conversion in the first cell results to be higher compared to

what happens downstream. The main effect is that, for temperatures slightly higher than the light-off one, the CO concentration is abated in the first cell more than it would be expected if one of the following cell were considered. As a result, the CO concentration downstream the first cell is reduced to a level at which, for the temperature considered, the reaction rate decreases, according to Eqn. 9, and the process returns to be kinetically limited in the following cells. *This effect can be also described on the basis of the Damköhler number, evaluated as the ratio between the reaction rate and the diffusion rate. The Da number calculated on the first Kelvin cell is around 1 for the temperature at which the light-off curve exhibits the transition to diffusion-controlled regime. On the other hand, for the same temperature, the Da number calculated for the downstream cells is below 1, because the flow development makes the CO gradients less significant. Therefore, in the second Kelvin cell, the conversion returns to be controlled by kinetics and, due to the lower CO concentration with respect to the first cell, the CO conversion rate decreases.* For that reason, the transition to the diffusion-controlled CO conversion on the whole catalytic surface occurs gradually and is completed at a temperature which is slightly higher than the light-off one.

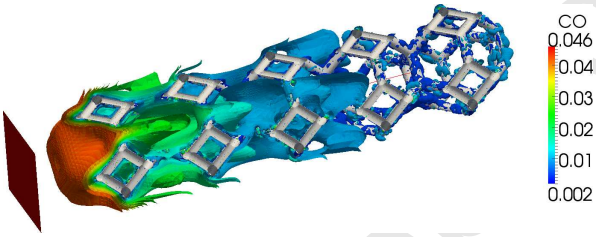

Figure 13: Foam-type reactor, sample E: CO iso-surfaces for an inlet CO mass fraction Y_{CO} = 4.6%, feed flow rate $Q = 3000\,Ncc/min$ and temperature $T = 620K$.

6. Conclusions

This paper describes the development of a CFD model for the simulation of catalytic surface reactions, with specific focus on the study of the conversion performances of open-cell foam substrates. The model was implemented on the basis of the open-source code OpenFOAM: a novel finite area solver was coupled to the standard finite volume solver in order to describe the conversion process, taking into account the diffusion of the reactants from the bulk to the washcoat and the catalytic reactions occurring on the surface. The modeling of the heterogeneous catalytic reactions was addressed with a simplified approach based on the Langmuir-Hinshelwood reaction model, able to predict the reaction rate on the basis of the surface conditions in terms of temperature, pressure and composition. Moreover, a steady-state algorithm was implemented under the assumption of negligible accumulation of reactants over the surface, in order to further reduce the computational effort required by the model, making it suitable for extensive simulation campaigns, which can involve the comparison of several substrates under different operating conditions. The model was firstly validated for the case of the oxidation of CO in a simple plate-type reactor under kinetically-controlled conditions, obtaining a satisfactory agreement between calculations and experiments. Then, the case of a reactor constituted by a foam substrate was considered and the full light-off curve was computed. In both the cases, the values of the constants adopted in the Langmuir-Hinshelwood reaction model were chosen a-priori on the basis of an experimental rate equation already published in a previous work. The agreement with experimental data is regarded as encouraging and compatible with the simplifications introduced in the model. In particular, the slight overestimation of the computed light-off curve is consistent with the assumption of uniform temperature of the solid matrix, which is actually not realistic for this specific case. In order to remove this assumption, a more sophisticated conjugate heat-transfer model is needed, in such a way to solve for the thermal balance of the solid foam matrix and determine the actual temperature distribution of the surface.

The proposed approach requires experimental reaction parameters to be available for the catalytic washcoat of interest. Thus, it is appropriate when the target of the investigation is the geometrical properties or operating conditions of the reactor, considering that the adoption of a detailed micro-kinetics model is computationally too expensive and is not justified according to the scope of the simulation. On the other hand, it cannot be applied for predicting the effects of the catalyst composition and loading and, at the present state, needs to be extended in order to consider the effects of intra-pore washcoat diffusion.

Acknowledgments

The authors gratefully acknowledge financial support from the Italian Ministry of Education, University and Research, Rome (MIUR, Progetti di Ricerca Scientifica di Rilevante Interesse Nazionale, prot. 2010XFT2BB), within the project IFOAMS: Intensification of Catalytic

Processes for Clean Energy, Low-Emission Transport and Sustainable Chemistry using Open-Cell Foams as Novel Advanced Structured Materials and from the Swiss Kompetenzzentrum für Energie und Mobilität CCEM via Project Number 704. Moreover, the contribution of Ing. Salvatore Indelicato, who performed the numerical simulations in the framework of his Msc thesis, is gratefully acknowledged.

List of Notations

$\alpha_{i,j}$	stoichiometric coefficient of the i-th species in the j-th reaction [−]
ΔL	mesh size [m]
$\mathfrak{Q}^{f\to w}$	energy source for FV-FA coupling - computed on the FV timestep [W]
$\mathfrak{R}_i^{f\to w}$	mass fraction source for FV-FA coupling - computed on the FV timestep [kg/s]
μ	viscosity [$Pa \cdot s$]
ρ	density [kg/m^3]
$\mathbf{U}$	velocity [m/s]
C	molar concentration [mol/m^3]
d_c	cell diameter [m]
d_s	strut diameter [m]
e	internal energy [J/kg]
H_r	reaction heat [W]
J_i	mass transfer between fluid and washcoat - computed on the FA timestep [kg/s]
k_a	adsorption kinetic constant
k_r	reaction kinetic constant
M_i	molecular weight of the i-th species [kg/mol]
p	pressure [Pa]
$Q^{f\to w}$	heat transfer between fluid and washcoat - computed on the FA timestep [W]
r_i	conversion rate for the i-th species [kg/s]
S_V	specific surface [m^2/m^3]
Y_i	mass fraction of the i-th species [-]

References

[1] K. Boomsma, D. Poulikakos, F. Zwick, Metal foams as compact high performance heat exchangers, Mechanics of Materials Vol. 35 (2003) 1161–1176.

[2] C. Thompson, P. Marín, F. Díez, S. Ordóñez, Evaluation of the use of ceramic foams as catalyst supports for reverse-flow combustors, Chemical Engineering Journal 221 (2013) 44–54.

[3] P. Dimopoulos Eggenschwiler, D. N. Tsinoglou, J. Seyfert, C. Bach, U. F. Vogt, M. Gorbar, Ceramic foam substrates for automotive catalyst applications. Fluid mechanic analysis, Experiments in Fluids (47, 2) (2009) 209–222.

[4] C. Bach, P. Dimopoulos Eggenschwiler, Ceramic Foam Catalyst Substrates for Diesel Oxidation Catalysts: Pollutant conversion and operational Issues, SAE Paper 2011-24-079.

[5] L. Giani, G. Groppi, E. Tronconi, Heat transfer characterization of metallic foams, Industrial and Engineering Chemistry Research 44 (24) (2005) 9078–9085.

[6] F. Patcas, G. Garrido, B. Kraushaar-Czarnetzki, CO oxidation over structured carriers: A comparison of ceramic foams, honeycombs and beads, Chemical Engineering Science 62 (15) (2007) 3984–3990.

[7] F. Lucci, A. Della Torre, G. Montenegro, P. Dimopoulos Eggenschwiler, On the catalytic performance of open cell structures versus honeycombs, Chemical Engineering Journal 264 (0) (2015) 514 – 521.

[8] K. Boomsma, D. Poulikakos, The Effects of Compression and Pore Size Variations on the Liquid Flow Characteristics in Metal Foams, Journal of Fluid Engineering Vol. 124 (2002) 263–272.

[9] Y. Peng, J. Richardson, Properties of ceramic foam catalyst supports: One-dimensional and two-dimensional heat transfer correlations, Applied Catalysis A: General 266 (2) (2004) 235–244.

[10] L. Giani, G. Groppi, E. Tronconi, Mass-transfer characterization of metallic foams as supports for structured catalysts, Industrial and Engineering Chemistry Research 44 (14) (2005) 4993–5002.

[11] G. Incera Garrido, B. Kraushaar-Czarnetzki, A general correlation for mass transfer in isotropic and anisotropic solid foams, Chemical Engineering Science 65 (6) (2010) 2255–2257.

[12] A. Della Torre, G. Montenegro, G. Tabor, M. Wears, CFD characterization of flow regimes inside open cell foam substrates, International Journal of Heat and Fluid Flow 50 (0) (2014) 72 – 82.

[13] *W. Regulski, J. Szumbarski, L. Laniewski-Wollk, K. Gumowski, J. Skibiński, M. Wichrowski, T. Wejrzanowski", Pressure drop in flow across ceramic foams – A numerical and experimental study, Chemical Engineering Science, 137 (2015) 320 – 337.*

[14] E. Bianchi, T. Heidig, C. G. Visconti, G. Groppi, H. Freund, E. Tronconi, An appraisal of the heat transfer properties of metallic open-cell foams for strongly exo-/endo-thermic catalytic processes in tubular reactors, Chemical Engineering Journal 198-199 (2012) 512–528.

[15] A. Diani, K. K. Bodla, L. Rossetto, S. V. Garimella, Numerical investigation of pressure drop and heat transfer through reconstructed metal foams and comparison against experiments, International Journal of Heat and Mass Transfer 88 (2015) 508 – 515. doi:http://dx.doi.org/10.1016/j.ijheatmasstransfer.2015.04.038.

[16] A. Della Torre, G. Montenegro, A. Onorati, G. Tabor, CFD Characterization of Pressure Drop and Heat Transfer Inside Porous Substrates, Energy Procedia 81 (2015) 836 – 845.

[17] F. Lucci, A. Della Torre, J. von Rickenbach, G. Montenegro, D. Poulikakos, P. Dimopoulos Eggenschwiler, Performance of randomized Kelvin cell structures as catalytic substrates: mass-transfer based analysis, Chemical Engineering Science 112 (0) (2014) 143 – 151.

[18] G. D. Wehinger, H. Heitmann, M. Kraume, An artificial structure modeler for 3D CFD simulations of catalytic foams, Chemical Engineering Journal 284 (2016) 543 – 556. doi:http://dx.doi.org/10.1016/j.cej.2015.09.014.
[19] G. Montenegro, A. Onorati, 1D Thermo-Fluid Dynamic Modeling of Reacting Flows inside Three-Way Catalytic Converters, SAE paper 2009-01-1510.
[20] D. Tsinoglou, P. Dimopoulos Eggenschwiler, T. Thurnheer, P. Hofer, A simplified model for natural-gas vehicle catalysts with honeycomb and foam substrates, Proceedings of the Institution of Mechanical Engineers, Part D: Journal of Automobile Engineering 223 (6) (2009) 819–834.
[21] M. E. Coltrin, R. J. Kee, F. M. Rupley, Surface chemkin. a general formalism and software for analyzing heterogeneous chemical kinetics at a gas-surface interface, International Journal of Chemical Kinetics 23 (12) (1991) 1111–1128.
[22] M. Salciccioli, M. Stamatakis, S. Caratzoulas, D. Vlachos, A review of multiscale modeling of metal-catalyzed reactions: Mechanism development for complexity and emergent behavior, Chemical Engineering Science 66 (19) (2011) 4319 – 4355.
[23] M. D. Smooke, R. E. Mitchell, D. E. Keyes, Numerical solution of two-dimensional axisymmetric laminar diffusion flames, Combustion Science and Technology 67 (4-6) (1986) 85–122.
[24] R. J. and Kee, J. A. Miller, A split-operator, finite-difference solution for axisymmetric laminar-jet biffusion flames, AIAA Journal 16 (2) (1978) 169–176.
[25] M. Maestri, A. Cuoci, Coupling CFD with detailed microkinetic modeling in heterogeneous catalysis, Chemical Engineering Science 96 (0) (2013) 106 – 117.
[26] H. G. Weller, G. Tabor, H. Jasak, C. Fureby, A Tensorial Approach to CFD using Object Orientated Techniques, Computers in Physics Vol. 12 (No. 6) (1998) 620.
[27] OpenFOAM documentation, Avaiable from: http://www.openfoam.org/docs/.
[28] S. V. Patankar, Numerical Heat Transfer and Fluid Flow, CRC Press, 1980.
[29] J.O. Hirschfelder, C.F. Curtiss, R.B. Bird, Molecular Theory of Gases and Liquids, Wiley, New York, 1954
[30] H. Karadeniz, C. Karakaya, S. Tischer, O. Deutschmann, Numerical modeling of stagnation-flows on porous catalytic surfaces: CO oxidation on Rh/Al2O3, Chemical Engineering Science 104 (2013) 899 – 907
[31] J. Rickenbach, F. Lucci, C. Narayanan, P. Dimopoulos Eggenschwiler, D. Poulikakos, Effect of washcoat diffusion resistance in foam based catalytic reactors, Chemical Engineering Journal 276 (2015) 388 – 397
[32] P. Baruah, Numerical solution of non-steady flows with variable specific heats and chemical reactions. Chapter 2 in: The Thermodynamics and Gas Dynamics of Internal Combustion Engines, MacGraw-Hill, 1986.
[33] G. Groppi, W. Ibashi, E. Tronconi, P. Forzatti, Structured reactors for kinetic measurements in catalytic combustion, Chemical Engineering Journal 82 (13) (2001) 57 – 71.
[34] E. Tronconi, G. Groppi, A study on the thermal behavior of structured plate-type catalysts with metallic supports for gas/solid exothermic reactions, Chemical Engineering Science 55 (24) (2000) 6021 – 6036.
[35] L. Giani, C. Cristiani, G. Groppi, E. Tronconi, Washcoating method for pd/-al2o3 deposition on metallic foams, Applied Catalysis B: Environmental 62 (12) (2006) 121 – 131.
[36] P. Habisreuther, N. Djordjevic, N. Zarzalis, Statistical distribution of residence time and tortuosity of flow through open-cell foams, Chemical Engineering Science 64 (23) (2009) 4943–4954.
[37] P. Du Plessis, A. Montillet, J. Comiti, J. Legrand, Pressure drop prediction for flow through high porosity metallic foams, Chemical Engineering Science 49 (21) (1994) 3545–3553.
[38] J. Skibinski, K. Cwieka, T. Kowalkowski, B. Wysocki, T. Wejrzanowski, K. J. Kurzydlowski, The influence of pore size variation on the pressure drop in open-cell foams, Materials & Design, 87 (2015) 650 – 655.
[39] L.L. Raja, R.J. Kee, O. Deutschmann, J. Warnatz, L.D. Schmidt, A critical evaluation of NavierStokes, boundary-layer, and plug-flow models of the flow and chemistry in a catalytic-combustion monolith, Catalysis Today 59 (2000) 47 – 60